Electronic Supplementary Information

Self-Assembly of Azamacrocyclic Ligands into Vesicular Structures: From Design to Functional Properties and Applications.

Mercy E. Arteaga-Vinza, Salvador Blasco, M. Paz Clares, M. Teresa Albelda, Juan. C. Frías, Lucía Bernat-Just, Phuong Linh Ta, Alicia López-Castellano, Jonathan L. Sessler and Enrique García-España.

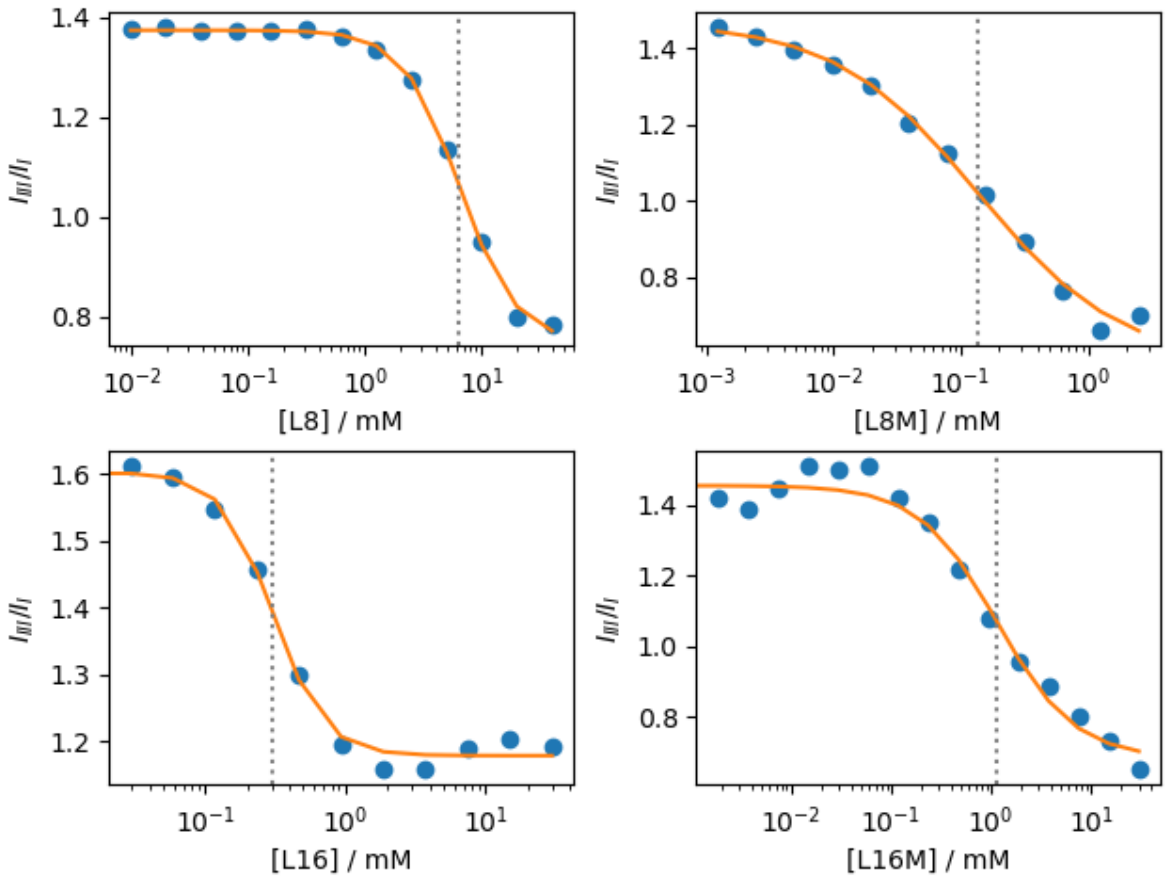

Figure S1: Critical micelle concentration data measured with the pyrene method in tris buffer 20mM at pH=7.4. The dotted line represents the calculated CMC.

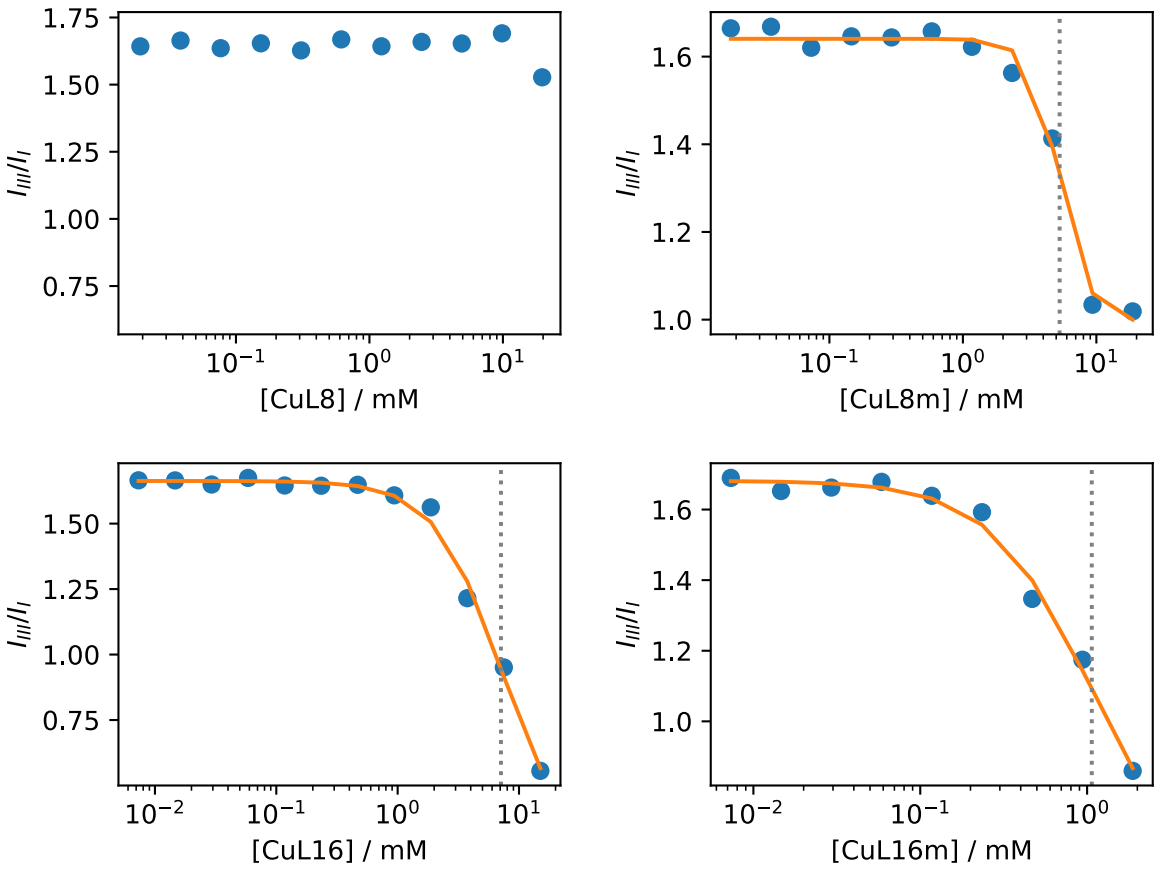

Figure S2: Critical micelle concentration data measured with the pyrene method in HEPES buffer 20mM at pH=7.4. The dotted line represents the calculated CMC.

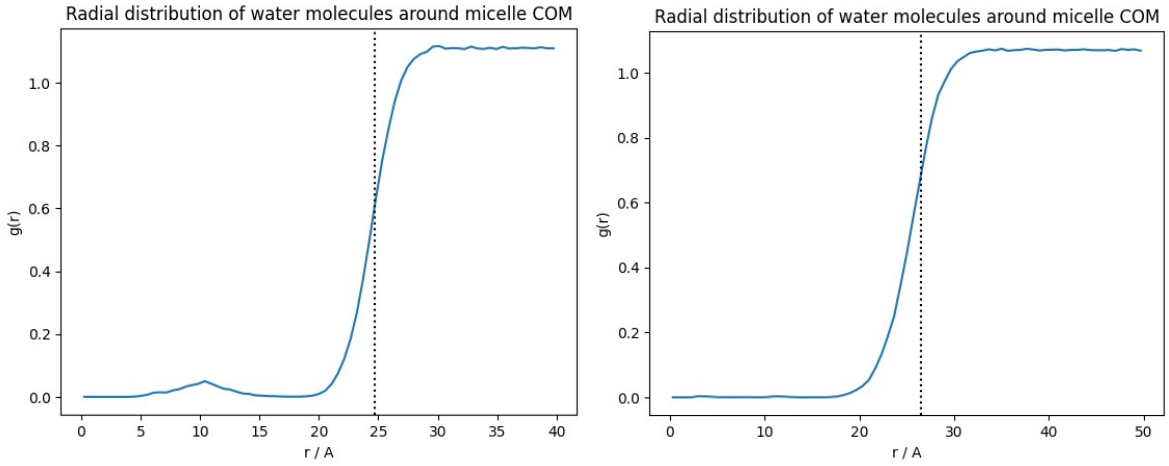

Figure S3: Radial distribution of water molecules with respect to the centre-of-mass of the micelle. **L8** (left) and **L8M** (right). The vertical dotted lines represent the calculated micellar radii.

Table S1: Crystallographic data

Composition	$C_{21}H_{39}CuN_5$, 2(ClO_4)
Formula weight / g·mol^{-1}	624.01
Size / mm	0.138×0.104×0.051
Space group	*P* 2_1/c
Unit cell	
• *a* / Å	20.919(5)
• *b* / Å	8.778(3)
• *c* / Å	14.947(4)
• *α* / degrees	90
• *β* / degrees	97.900(9)
• *y* / degrees	90
• *V* / Å3	2718.7(12)
Density / g·cm^{-3}	1.53
Z	4
μ / mm^{-1}	1.05
F000	1308
Diffraction Limits	29 ≤ h ≤ −29
	12 ≤ k ≤ −12
	21 ≤ l ≤ −21
R(int)	0.1042
R(sigma)	0.0575
Reflections	
• Collected	58548
• Unique	8299
Parameters	365
Constraints	0
Restraints	1
*R*1	
• total	0.1138
• $F^2 > 2\sigma(F^2)$	0.0706
w*R*2	
• total	0.1911
• $F^2 > 2\sigma(F^2)$	0.1661
Goodness of Fit	1.029

Table S2: Bond distances (in angstrom) and angles (in degrees) for crystal structure Cu**L8** (this work) and Cu**L** for comparison (from *Inorg Chem* 2007, 46(14), 5707-5719). The crystal Cu**L** contains two separate moieties, both of which are shown here, and the atom labelling in the referenced paper do not match those for Cu**L8** in this work, but in this table they have been rearranged so that the number corresponds to the analog atom in the Cu**L8** crystal.

	Cu**L8**	Cu**L**	
Cu1–N1	1.930(3)	1.950(9)	1.938(8)
Cu1–N2	2.108(3)	2.074(9)	2.116(8)
Cu1–N3	2.200(3)	2.189(9)	2.231(8)
Cu1–N4	2.125(3)	2.097(9)	2.104(8)
Cu1–N5	2.005(3)	2.052(9)	1.997(8)
N1–Cu1–N2	81.35(13)	81.0(4)	81.5(3)
N1–Cu1–N3	100.12(13)	119.5(3)	99.4(3)
N1–Cu1–N4	81.67(13)	82.3(4)	82.3(4)
N2–Cu1–N3	84.29(12)	83.3(3)	82.5(3)
N4–Cu1–N3	83.48(12)	84.7(3)	84.5(3)
N5–Cu1–N2	97.13(14)	103.5(4)	99.7(3)
N5–Cu1–N3	85.15(14)	82.7(3)	82.7(3)
N5–Cu1–N4	101.21(14)	100.8(4)	98.0(3)
τ_5	0.289	0.267	0.108

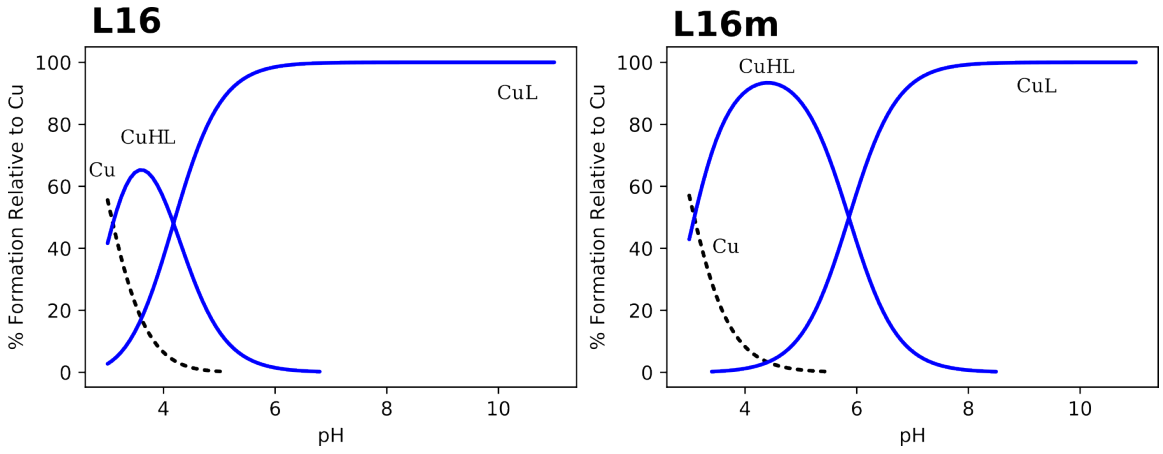

Figure S4: Distribution diagrams for the systems referred to as Cu^{2+}-**L16** and Cu^{2+}-**L16m** as a function of pH. The metal cation-ligand ratio was 1:1 ([L]=[Cu^{2+}] = 10^{-3} M). Dashed lines represents the molar fraction of free Cu^{2+}.

Figure S5: ^{1}H-NMR spectrum for **L8**

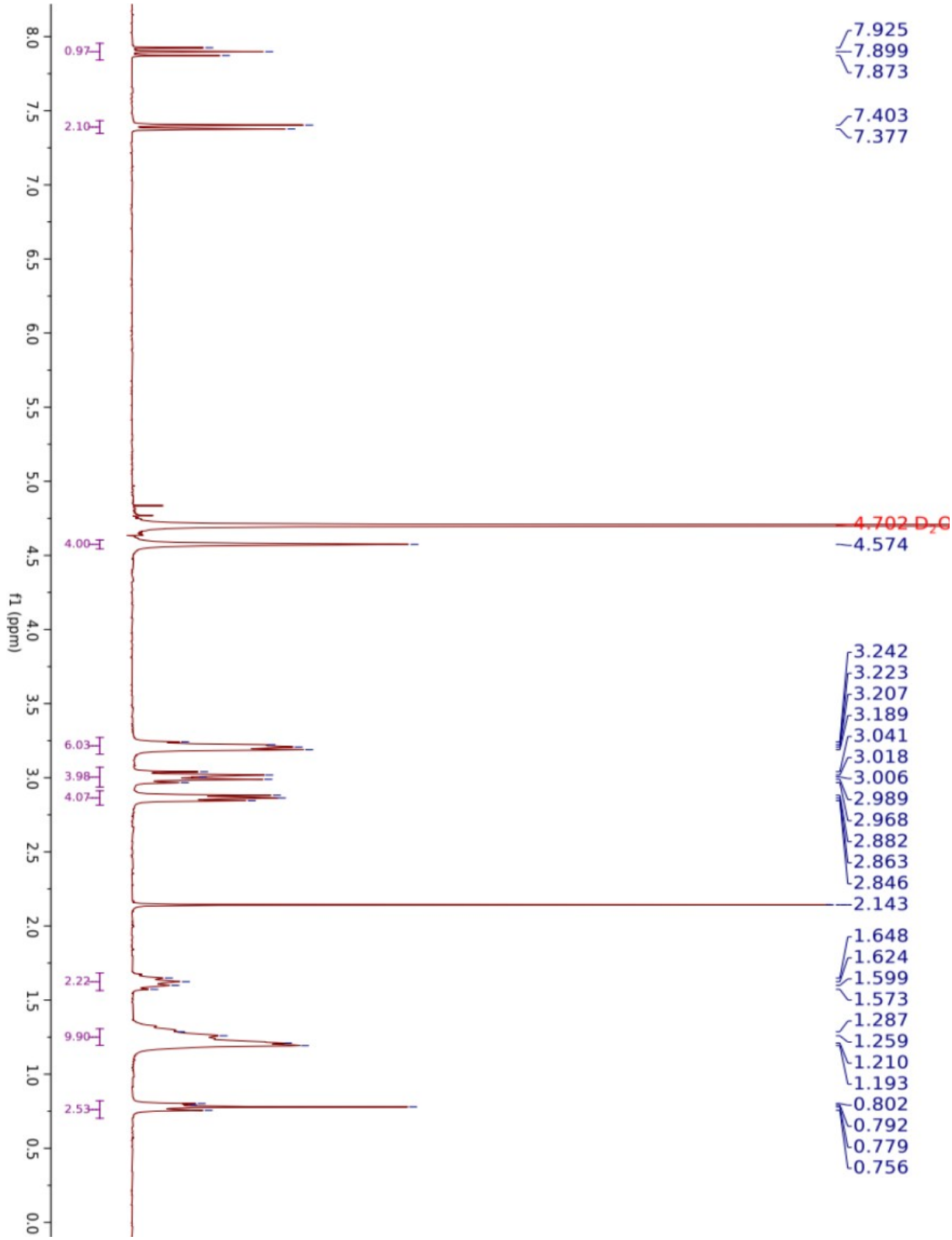

Figure S6: ^{13}C-NMR spectrum for **L8**

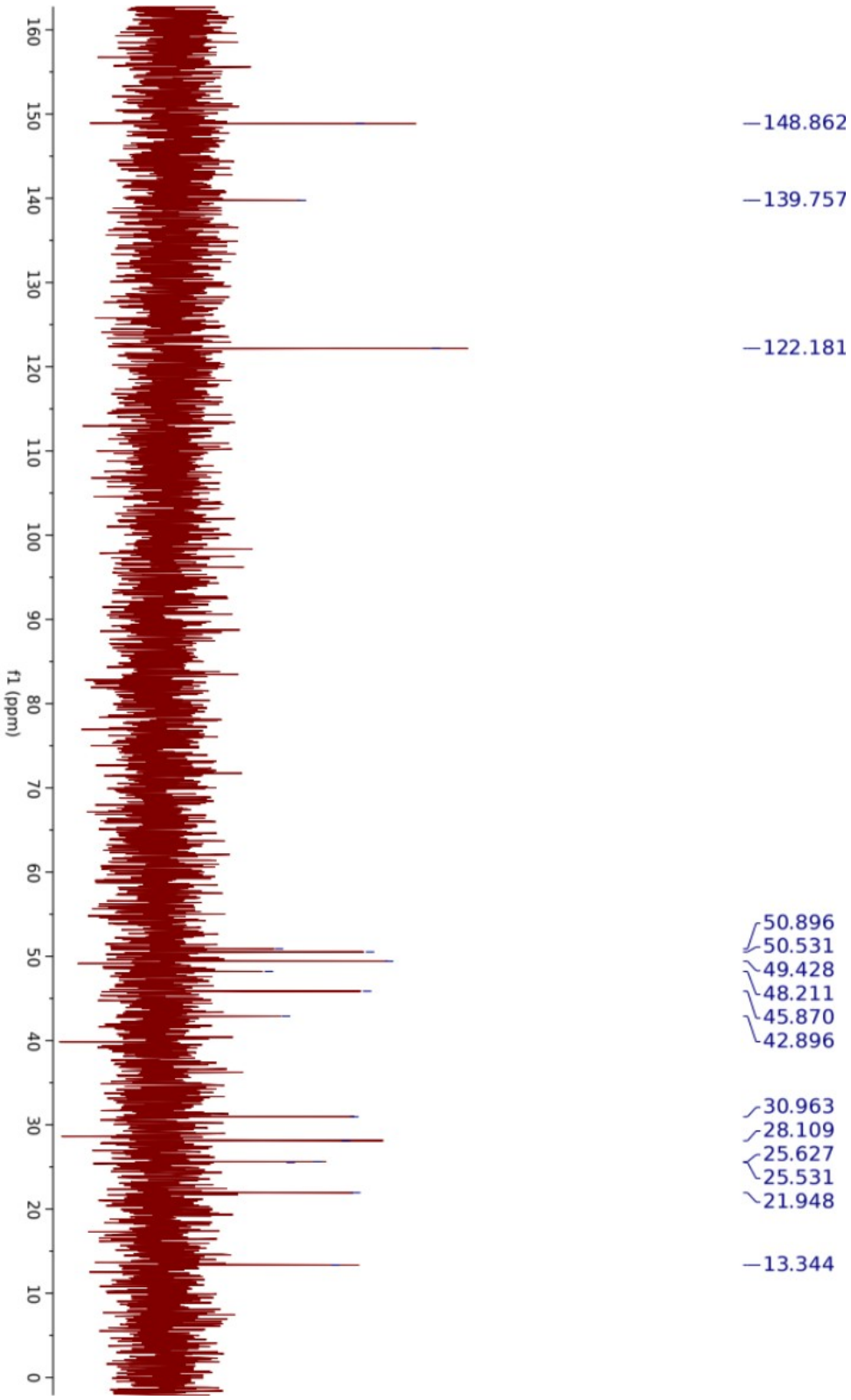

Figure S7: ^{1}H-NMR spectrum for **L8Ts**

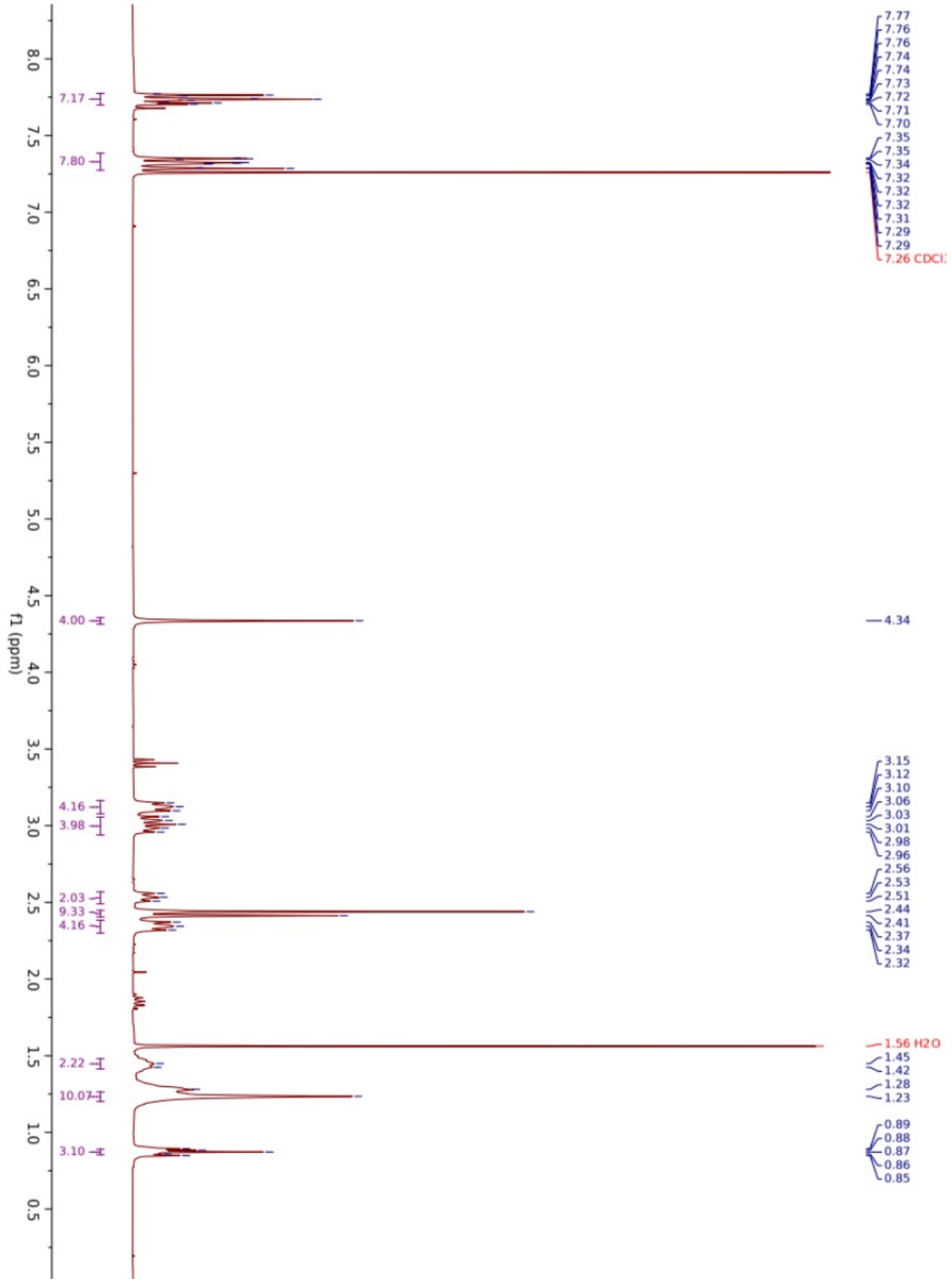

Figure S8: ^{13}C-NMR spectrum for **L8Ts**

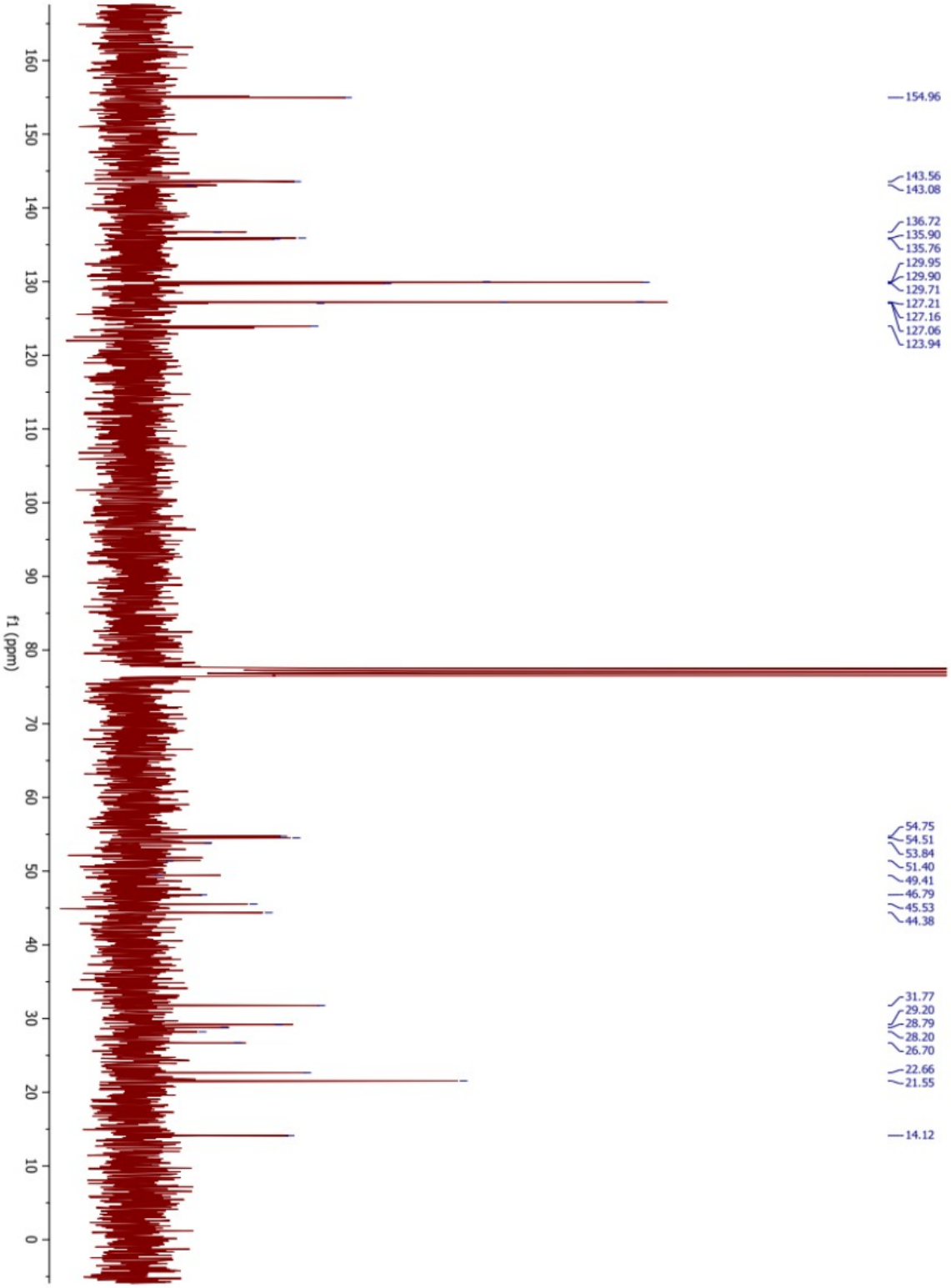

Figure S9: ^{1}H-NMR spectrum for **L8m**

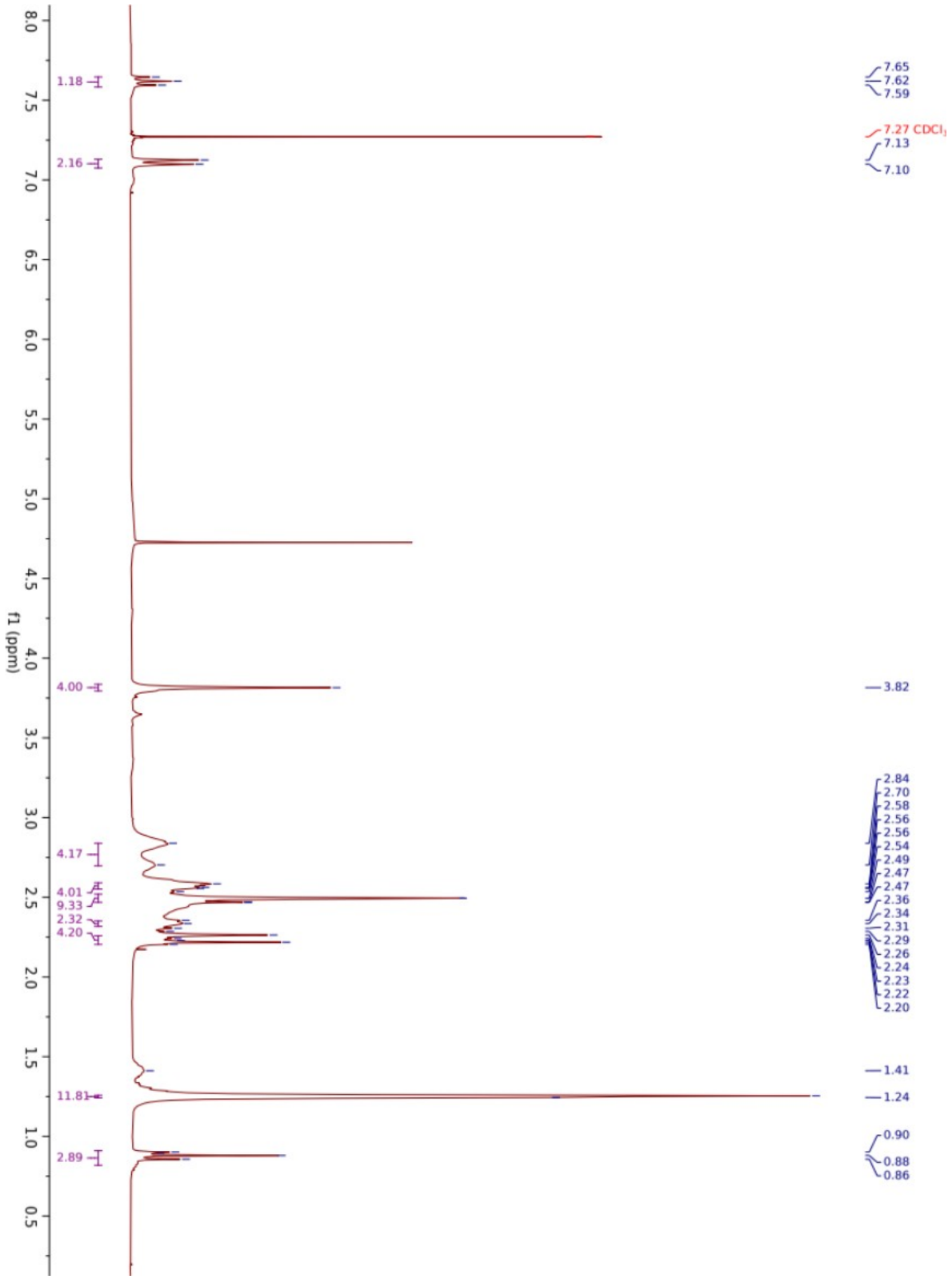

Figure S10: ^{13}C-NMR spectrum for **L8m**

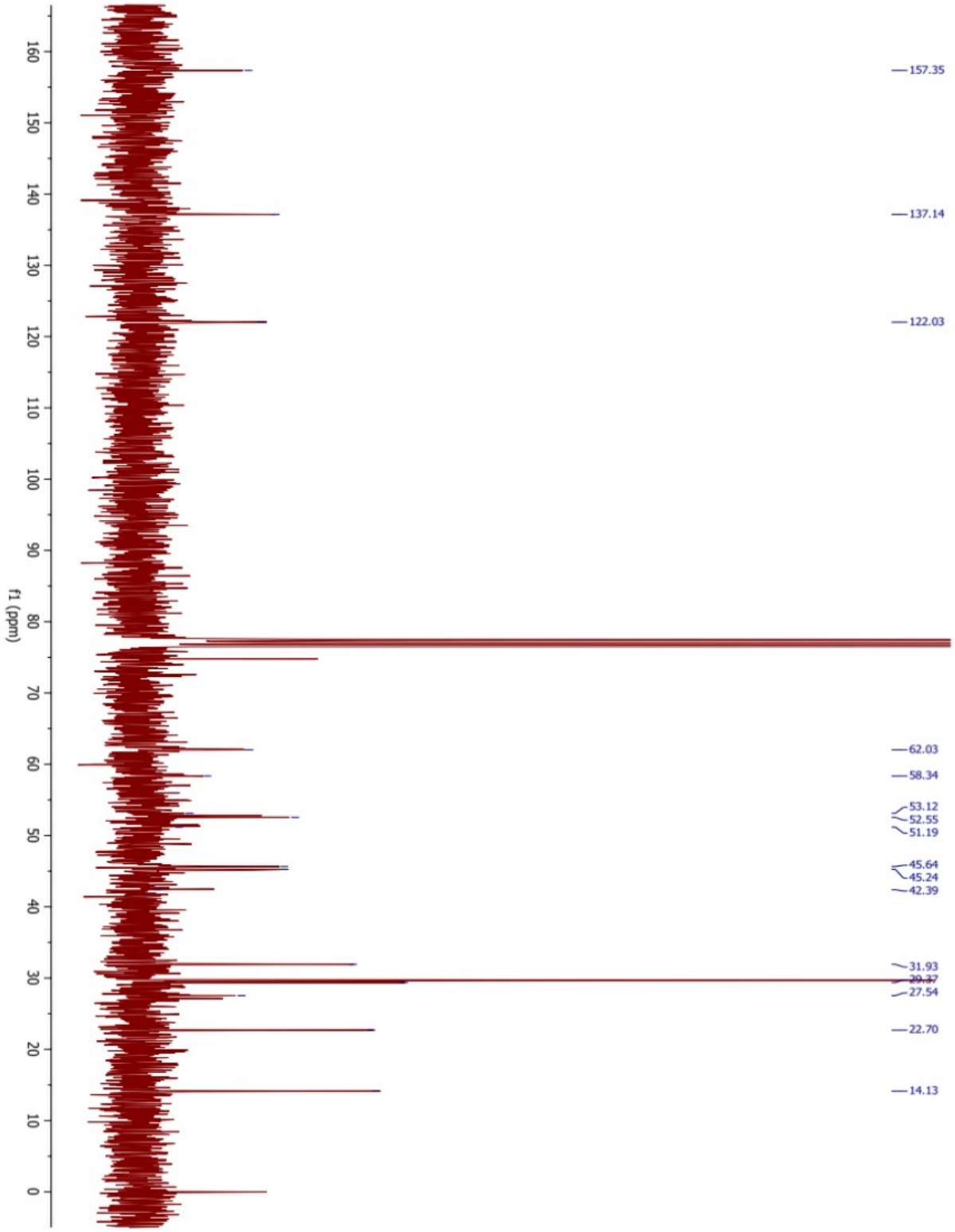

Figure S11: ^{1}H-NMR spectrum for **L16Ts**

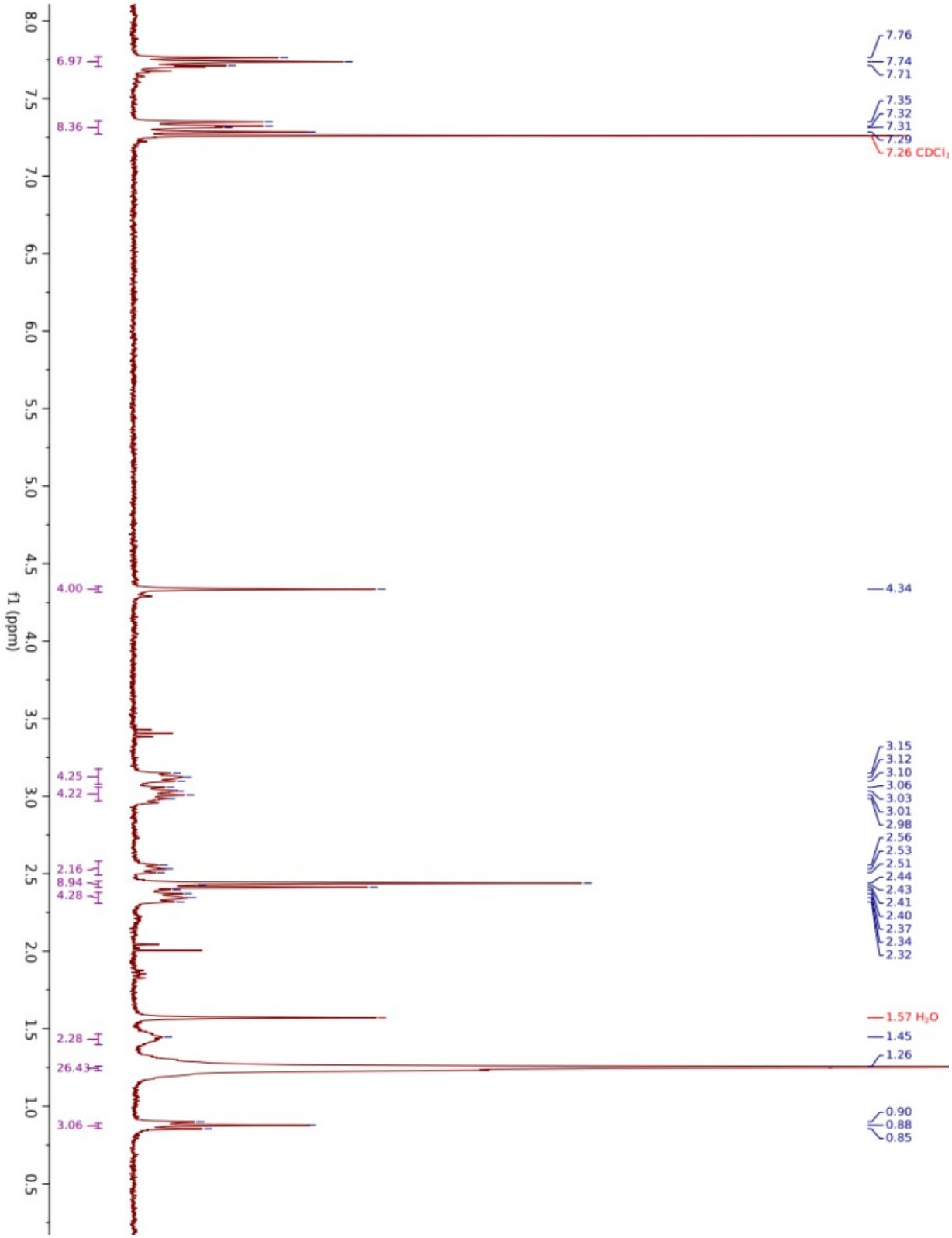

Figure S12: ^{13}C-NMR spectrum for **L16Ts**

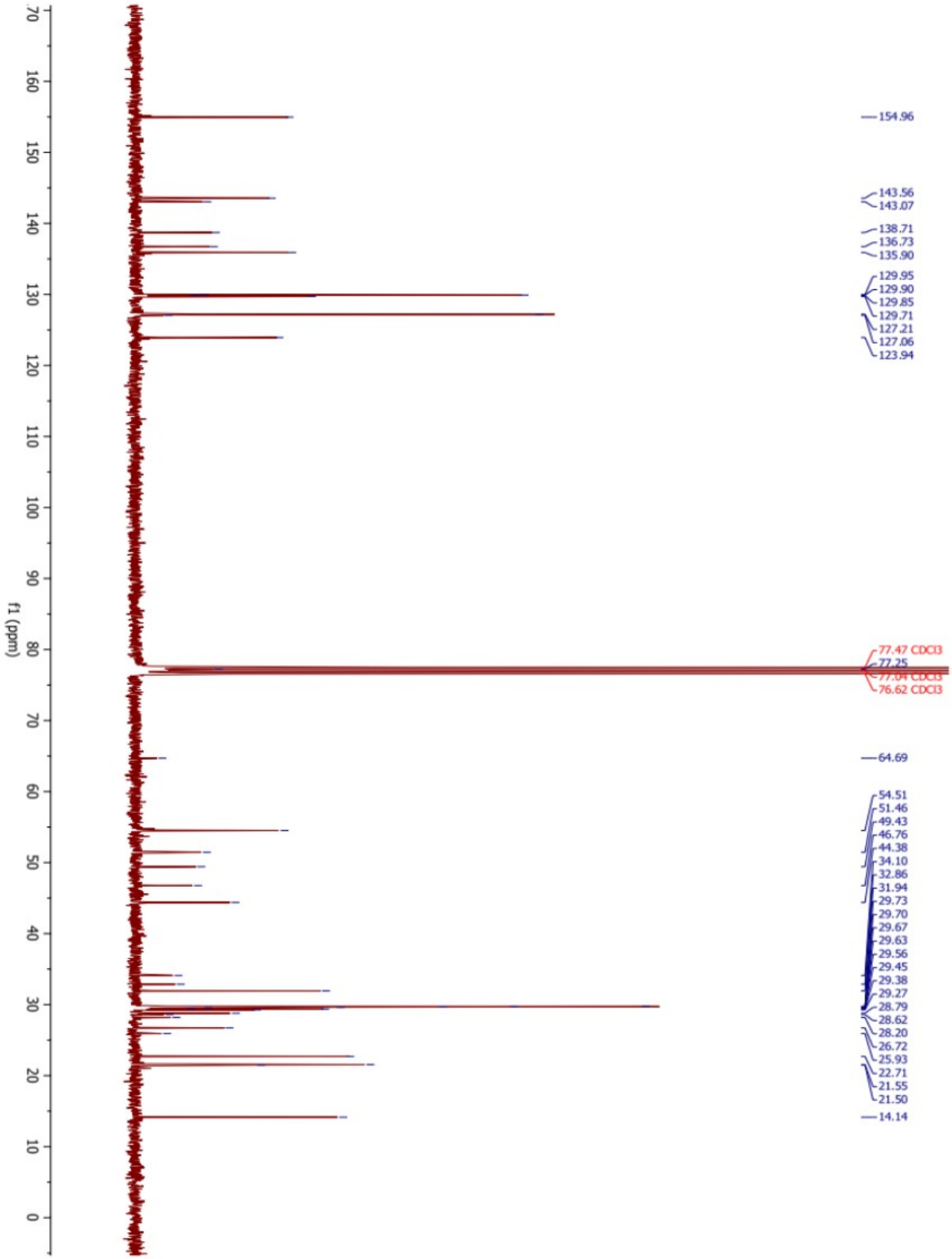

Figure S13: ^{1}H-NMR spectrum for **L16**

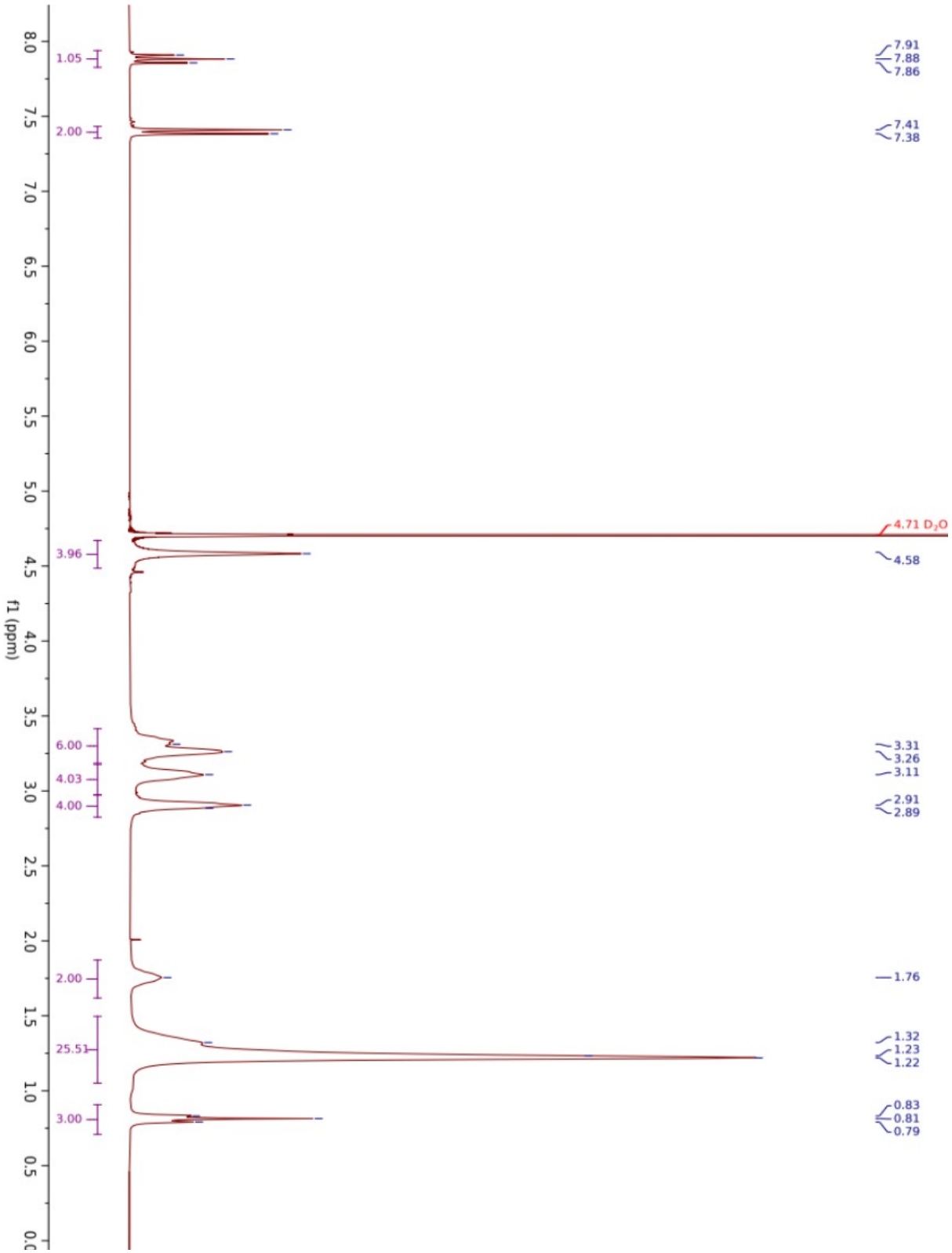

Figure S14: ^{13}C-NMR spectrum for **L16**

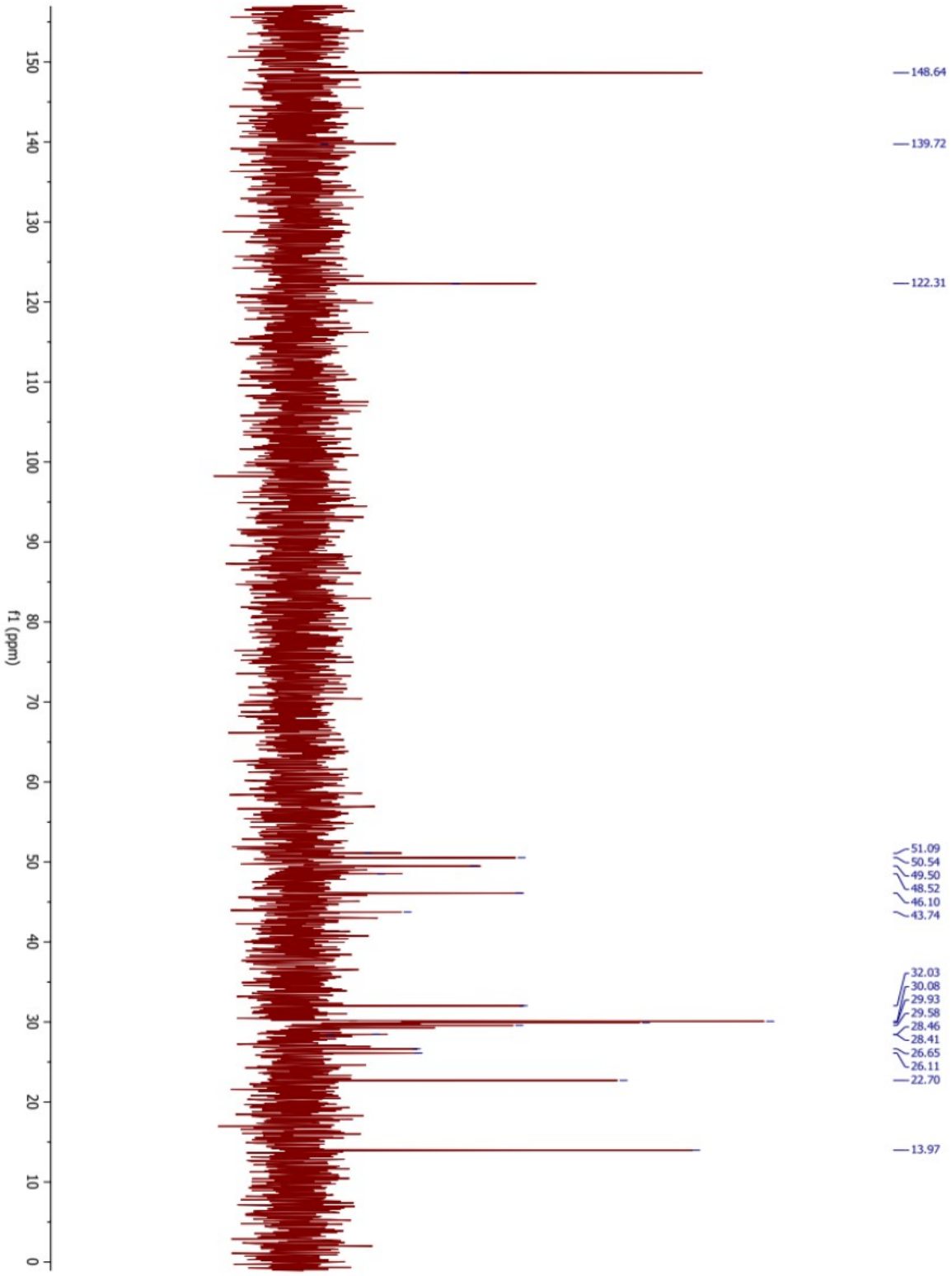

Figure S15: ^{1}H-NMR spectrum for **L16m**

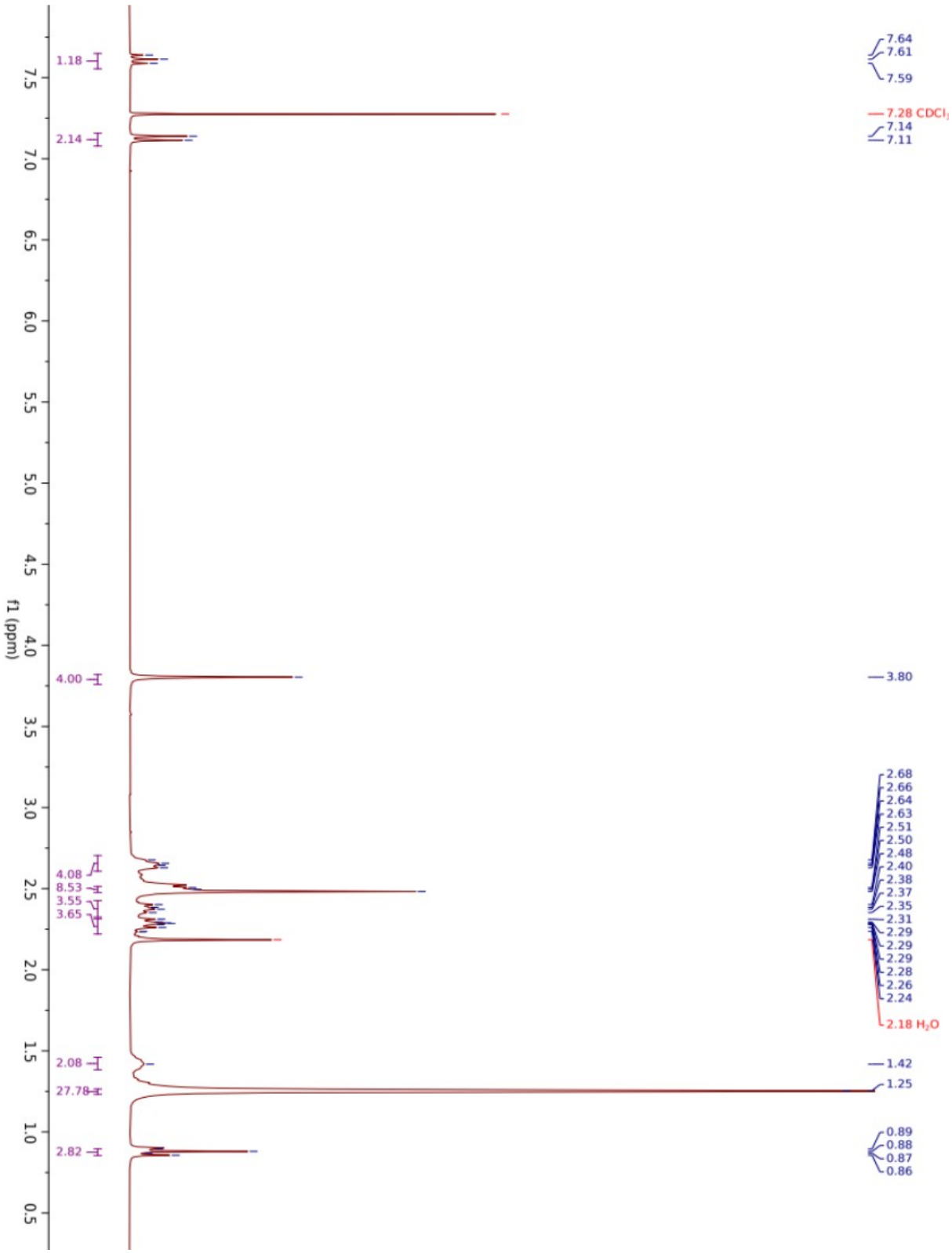

Figure S16: ^{13}C-NMR spectrum for **L16m**

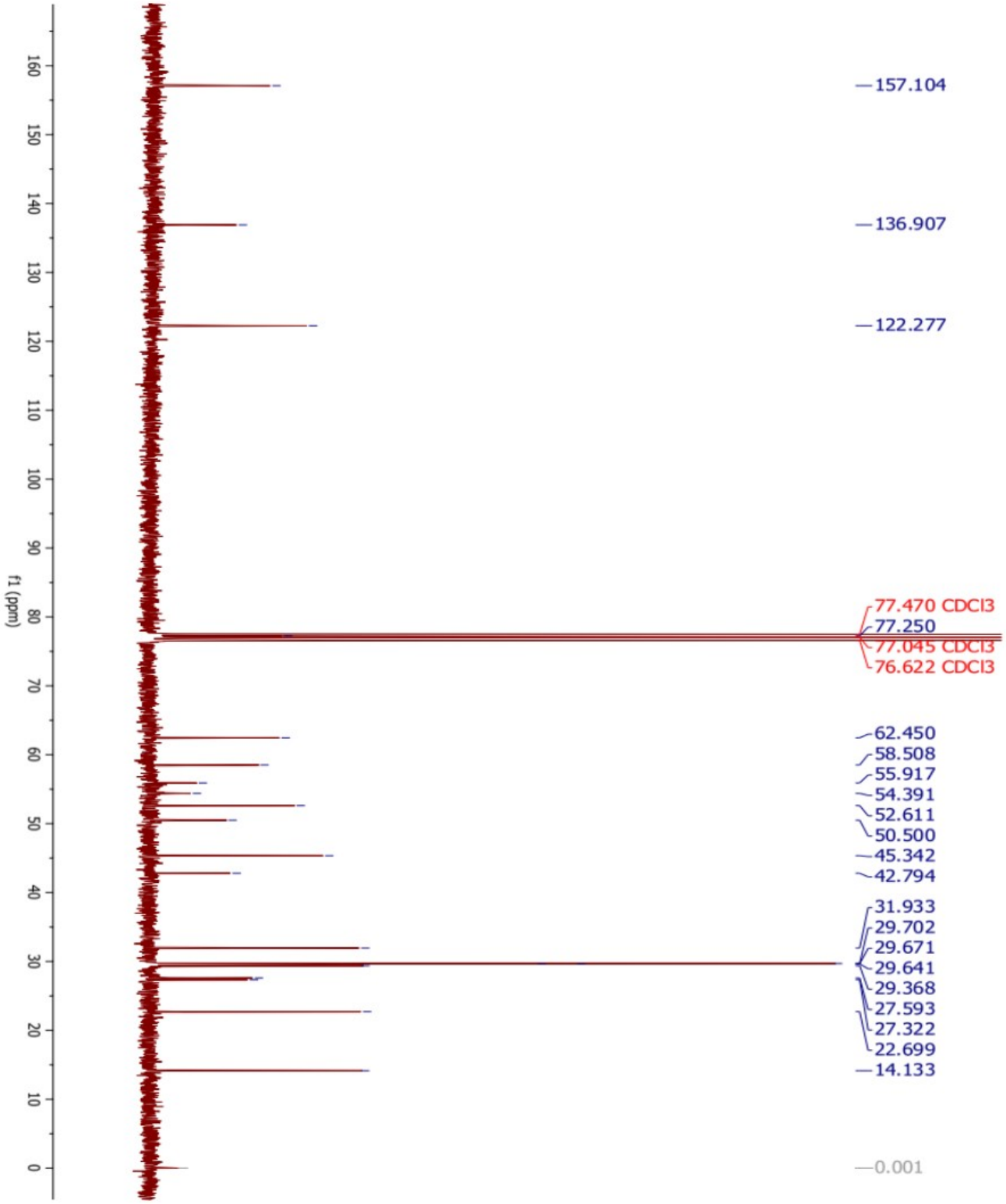

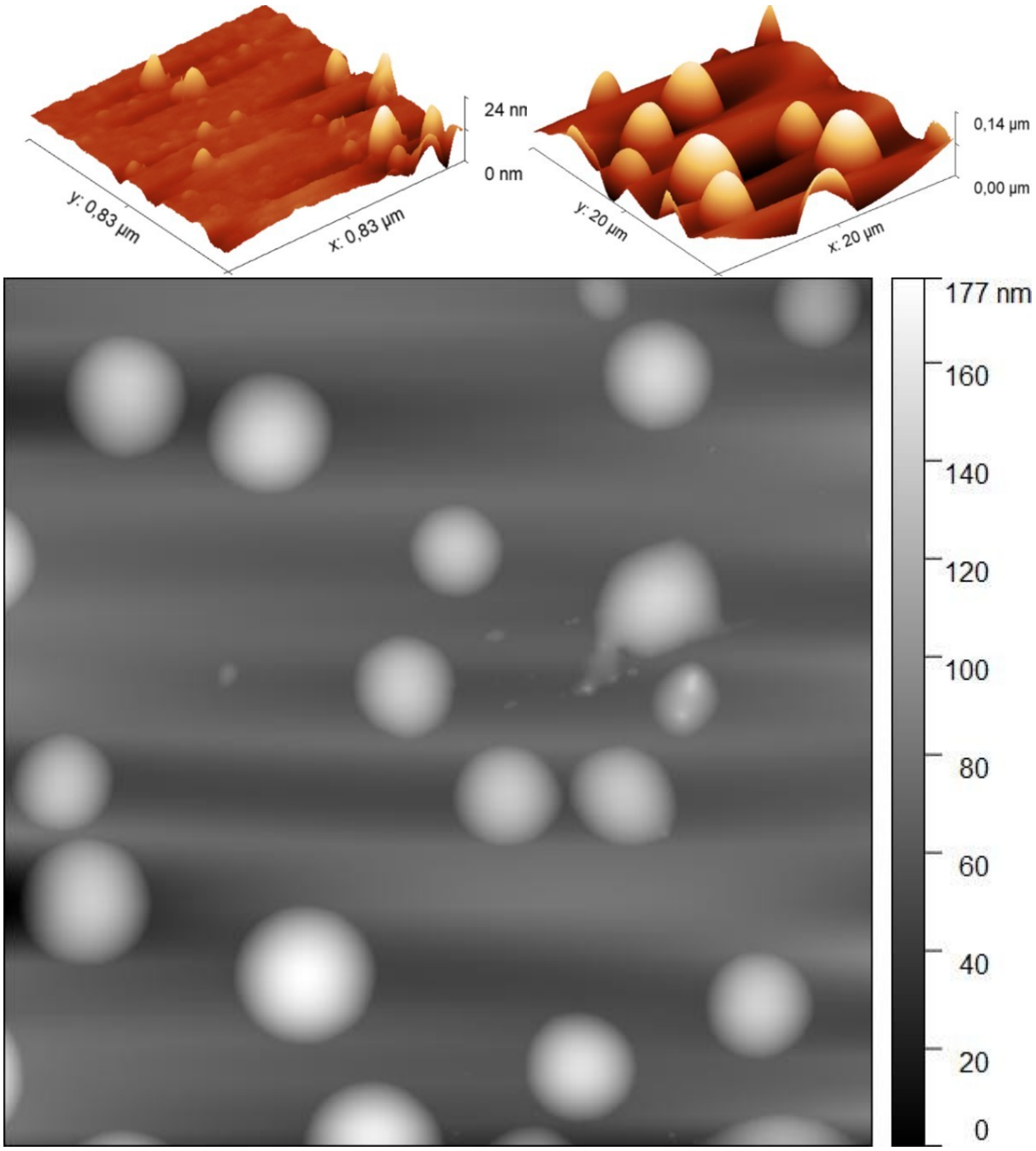

Figure S17: AFM images of L8 (top left) and L8m (top right and bottom).